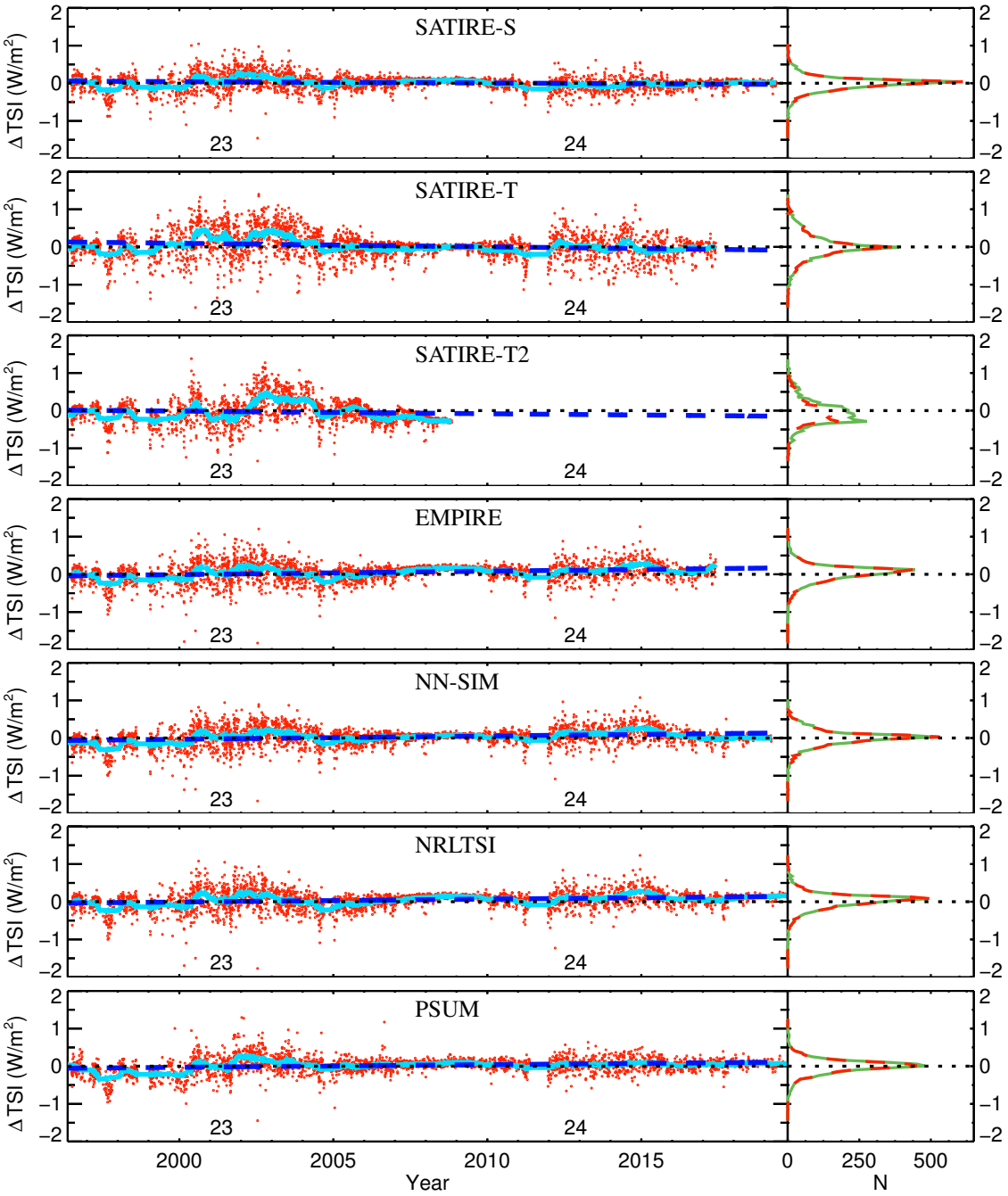

Fig. A.2. Same as Fig. A.1 but showing the differences to the SATIRE-S, SATIRE-T, SATIRE-T2, EMPIRE, NN-SIM, NRLTSI, and PSUM reconstructed TSI series.

Appendix B: Effect of bandwidth on the contribution of sunspots to faculae filling factors

To understand whether the contribution of sunspots to the derived facular filling factors is affected by the bandwidth of the Ca II K observations, we repeated the analysis presented in Sect. 4.2 for the datasets taken with different filters. Figures B.1 and B.2 show the results for the MD1 and SF datasets, which are the two extreme cases of bandwidth analysed here (narrowest and broadest, respectively). We note that B_{sat} for the three TSI reconstructions from MD1 and SF Ca II K data used for this test was determined by considering the same period, which is limited to the period after September 1997 as dictated by the availability of red-continuum Rome/PSPT observations. This differs to the results presented in the main text with MD1 and SF where the entire period since 1978 and 1992, respectively, was used to set B_{sat}. For all archives, we report a marginal improvement in the linear correlation and the RMS differences between the reconstructed TSI and the PMOD TSI series when the actual locations of sunspots are used to correct the facular filling factors compared to the case that they are not corrected. However, the improvement is rather minor, as already reported for RP data in Sect. 4.2. This reinforces our conclusion that the information on the sunspot filling factors can be determined from an independent series, such as that of Mandal et al. (2020), without applying any correction to the facular filling factors. As mentioned before, this is an important result since most historical datasets do not have co-temporal white light or continuum observations to provide the information on sunspots.

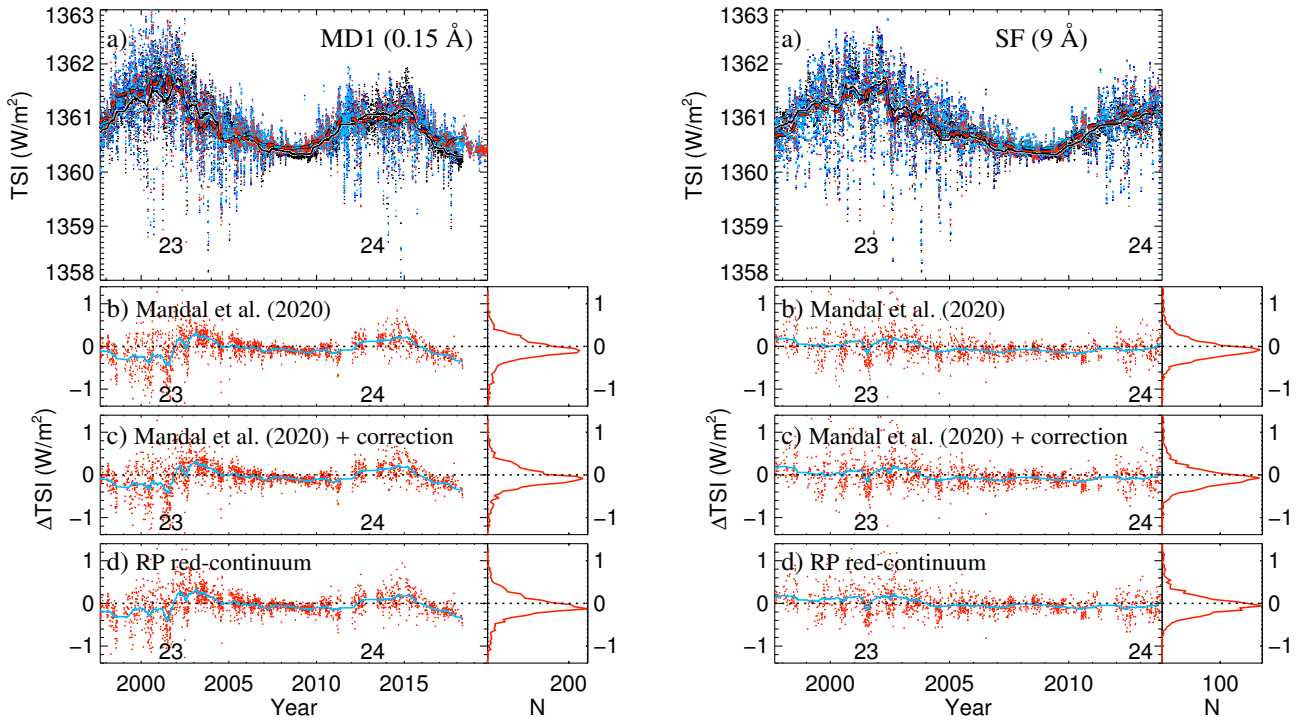

Fig. B.1. TSI reconstructed with MD1 (left panels) and SF (right panels) Ca II K data as a function of time (a) and difference of TSI reconstructions to the PMOD TSI composite (b–d) when using different approaches to account for the sunspots: using the Mandal et al. (2020) series to get the sunspot filling factors (light blue in panel a and red in panel b); using the Mandal et al. (2020) series to get the sunspot filling factors which were also subtracted from those of faculae (blue in panel a and red in panel c); using full-disc Rome/PSPT red continuum data (red in panel a and d) to get the sunspot filling factors (see Sect. 4.2 for more information). The differences are shown only for the common days in all series. Also shown in panel a is the PMOD TSI composite (black). Thick lines show 81-day running mean values. The right part of the lower panels show the distributions of the differences in bins of 0.05 Wm^{-2}.

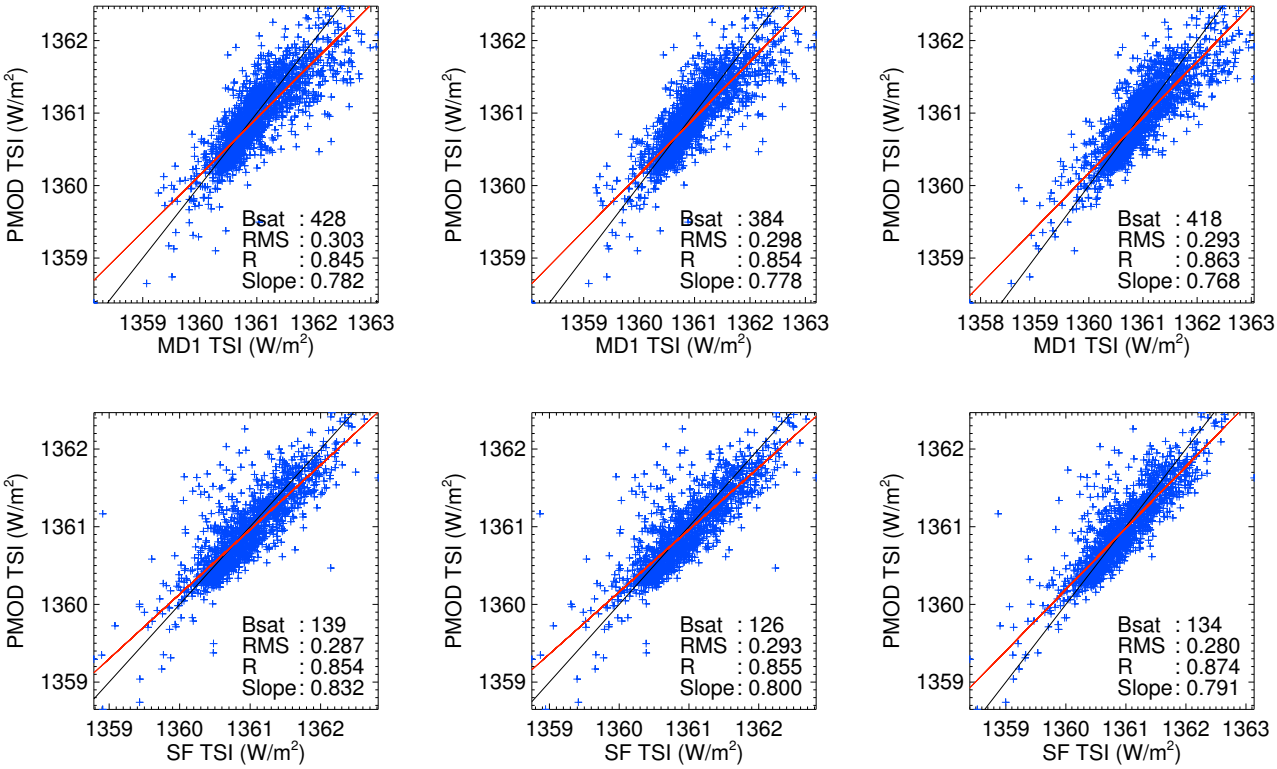

Fig. B.2. TSI reconstructed from MD1 (top row) and SF (bottom row) Ca II K images versus the PMOD TSI composite. *Left:* Sunspot information taken from Mandal et al. (2020) without any correction to the faculae filling factors due to sunspots; *Middle:* Sunspot information taken from Mandal et al. (2020) and the sunspot filling factors are subtracted from the facular ones; *Right:* Sunspot information is derived from the full-disc RP red-continuum images. The red lines show linear fits to the data, while the black lines have a slope of unity. Also listed in each panel are the B_{sat} (in G), RMS difference (in W/m^2), the linear correlation coefficient, and the slope of the linear fit.